Biosensors and Bioelectronics 130 (2019) 315–321

Contents lists available at ScienceDirect

Biosensors and Bioelectronics

journal homepage: www.elsevier.com/locate/bios

Simultaneous voltammetric determination of acetaminophen and isoniazid using MXene modified screen-printed electrode

Yu Zhang[a], Xiantao Jiang[c], Junjie Zhang[a], Han Zhang[c], Yingchun Li[a,b,*]

[a] Key Laboratory of Xinjiang Phytomedicine Resources and Utilization, Ministry of Education, School of Pharmacy, Shihezi University, Shihezi 832000, China
[b] College of Science, Harbin Institute of Technology, Shenzhen 518055, China
[c] Collaborative Innovation Center for Optoelectronic Science & Technology, International Collaborative Laboratory of 2D Materials for Optoelectronics Science and Technology of Ministry of Education, College of Optoelectronic Engineering, Shenzhen University, Shenzhen 518060, China

ARTICLE INFO

Keywords:
Simultaneous detection
MXene $Ti_3C_2T_x$
2D nanomaterial
Acetaminophen
Isoniazid
Electrochemical sensor

ABSTRACT

Determination of hepatotoxic drugs is critical for both clinical diagnosis and quantity control of their pharmaceutical formulations. In this work, a facile and sensitive sensor based on MXene modified screen-printed electrode (MXene/SPE) has been developed for detection of acetaminophen (ACOP) and isoniazid (INZ), which are two commonly used drugs but might induce liver damage in certain circumstances. MXene showed excellent electrocatalytic activity toward the oxidation of ACOP and INZ compared with bare SPE in 0.1 M H_2SO_4, and the separated oxidation peak potentials ensured simultaneous detection of the targets with wide linear ranges from 0.25 to 2000 μM for ACOP and 0.1–4.6 mM for INZ. The detection limits of ACOP and INZ were 0.048 μM and 0.064 mM, respectively. (S/N = 3). MXene/SPE exhibits good stability, reproducibility and repeatability, and the method has been successfully applied for detection of ACOP and INZ in their pharmaceutical and biological samples with satisfactory recovery.

1. Introduction

Drug-induced hepatotoxicity is a frequent cause of liver injury, since liver is the major organ participating in transformation of medicines and their metabolites, which is sometimes accompanied by direct or indirect toxic damage to the liver cells. Certain medicinal agents, when taken in overdoses and sometimes even within therapeutic ranges, may injure the organ. Drug-induced hepatotoxicity is also the most common reason for a drug to be withdrawn from the market (Lawrence Goldkind and Loren Laine, 2010).

More than 900 drugs have been implicated in causing liver injury (Kullakublick et al., 2017), among them, acetaminophen (ACOP), also known as paracetamol, is a classical dose-dependent hepatotoxin that is responsible for almost 50% of all acute liver failure cases worldwide (Ampolson, 2006). ACOP is a medicine in widespread use for pain and fever treatment, and perceived to be an effective and safe drug when taken in recommended dose. Excessive consumption of ACOP (daily maximum of 4 g/day) may induce hepatotoxicity. In this circumstance, a toxic metabolite (N-acetyl-p-benzoquinone imine) produced by cytochrome P-450 enzymes could overwhelm its detoxification process and may result in severe liver cell damage. When plasma concentration of ACOP over 200 μg/mL (about 1.3 mM), patients can be diagnosed as ACOP toxicosis (Rumack et al., 2012). However, since ACOP poisoning is characteristic of acute occurrence and concealment of the early symptoms, it is easy to miss the diagnosis and delay treatment and rescue work. Thus, establishment of a rapid, simple and accurate ACOP assay tool with applicability for point of care testing and early toxicity assessment is in a pressing need.

Antibacterial drugs are another common class of hepatotoxic drugs (Leitner et al., 2010). Since antibacterials and ACOP are so common and available drugs in daily life, there is a growing concern over liver damage caused by a combination of ACOP and antibacterial drugs. Isoniazide (INZ) is known as the first-line drug against tuberculosis, which is associated with mild elevation of liver enzymes in up to 20% of patients and severe hepatotoxicity in 1–2% of patients (Nolan et al., 1999). Pretreatment with INZ could increase the risk of ACOP-induced hepatic necrosis by 85% (Epstein et al., 2012). Therefore, patients taking INZ and ACOP at the same time are at increased risk of liver damage and suggested to dose with caution and monitor hepatic function at regular interval. Consequently, developing a simple, sensitive and selective method for simultaneous detection of ACOP and INZ is highly desirable.

Several analytical methods have been developed for quantifying ACOP and INZ, including UV–visible spectrophotometry, high

* Corresponding author at: College of Science, Harbin Institute of Technology, Shenzhen 518055, China.
E-mail address: liyingchun@hit.edu.cn (Y. Li).

https://doi.org/10.1016/j.bios.2019.01.043
Received 22 October 2018; Received in revised form 24 December 2018; Accepted 16 January 2019
Available online 29 January 2019
0956-5663/

performance liquid chromatography, titrimetry, flow injection analysis, capillary electrophoresis and electrochemical methods (Espinosa et al., 2006; Fernandes et al., 2017; Shahrokhian and Amiri, 2007; Tan et al., 2018). Most of the approaches are relatively time consuming and need specialized person to conduct the tests. In comparison, electrochemical analysis has unique features in respects of fast response, easy handling, low cost, organic solvents free, and easy miniaturization (Cheng et al., 2015).

Screen-printed electrode (SPE) is suitable to make effective, versatile and low-cost miniature-sized sensors. Besides, its microliter-level demand of sample and good repeatability makes it an ideal analytical platform for point-of-care testing (Ahmed et al., 2015). In order to improve sensitivity and detection capacity of SPE, we employed self synthesized MXene as coating matrix for modification of SPE. MXene is a new class of 2D nanomaterial that was first reported in 2011 (Lukatskaya et al., 2013). Since then it has attracted considerable attention in various research fields (Tang et al., 2012; Zhu et al., 2017). The general formula of MXene is $M_{n+1}X_nT_x$, where M is an early transition metal, X is C and/or N, T is the surface terminations (H, O or F), and n = 1, 2, or 3. It has many outstanding merits including large surface area, excellent electrical conductivity, compatibility with water and organic solvent, and easy fabrication at room temperatur, which are ascribed to its layered architecture, existence of metal in its components, presence of negative charges on the surface. Based on its unique structural, electrical and chemical properties, MXene shows great potential in many applications, such as catalysts (Gao et al., 2017), super capacitors (Rakhi et al., 2015) and sensors (Kumar et al., 2018). The most studied form of MXene is $Ti_3C_2T_x$ due to its facile synthesis, high mechanical strength, good catalysis properties and hydrophilicity (Hantanasirisakul et al., 2016). For all we know, only few literatures using MXene for sensing application are reported, and there is still abundant room to explore and extend the usage of MXene in sensing and sensor-related fields.

Herein, we developed a new electrochemical sensing platform by integrating SPE and MXene for simultaneous and selective determination of ACOP and INZ. Delaminated $Ti_3C_2T_x$ solution was drop casted on SPE surface and acted as signal enhancing matrix. The electrochemical performance of SPE/MXene was investigated. Furthermore, the developed sensor was successfully applied to determine ACOP and INZ in their individual pharmaceutical formulations, and simultaneous detection of the two target molecules in human fluids was also performed (Scheme 1).

2. Experimental

2.1. Reagents and Apparatus

Acetaminophen (ACOP) and isoniazid (INZ) were purchased from Adamas Reagent Co. Ltd. (Shanghai, China). ACOP tablets (500 mg) were bought from Sinopharm Group Guangdong Medi-World Pharnaceutical Co. Ltd. (Guangdong, China), and INZ tablets (100 mg) were bought from Shenyang Hongqi Pharmaceutical Co. Ltd (Shenyang, China). Sulfuric acid (98%) was purchased from Zhuhai HuaChengDa Chemical Co. Ltd. (Guangdong, China). Other chemicals, such as $K_3[Fe(CN)_6]$, $K_4[Fe(CN)_6]\cdot 3H_2O$, NaOH, and KCl were obtained from Guangfu Tech. Co. Ltd. (Tianjin, China). All the other reagents were of analytical grade and the solutions were prepared with ultra-pure water (Milli-Q, Millipore). Ti_3AlC_2 powder (99%, average particle size ≤ 30 μm) was purchased from Forsman Scientific Co. Ltd. (Beijing, China).

All electrochemical measurements were carried out with a computer-controlled CHI 660E electrochemical workstation (ChenHua Instruments Co., Shanghai, China). Three-electrode screen-printed electrodes (SPEs) were purchased from Zensor Research & Development (Taiwan, China). Deaerated H_2SO_4 (0.1 M) was used as the electrolyte. Electrochemical impedance spectroscopy (EIS) experiments were conducted at a potential of 224 mV in the frequency range from 0.01 Hz to 100 kHz with a signal amplitude of 5 mV. Surface morphologies of SPE/MXene were characterized by scanning electron microscopy (SEM, Zeiss Supra 55VP). Energy dispersive spectrometry (EDS) was conducted with a Nova Nano FESEM 450 at 10 kV equipped with Energy Dispersive X-ray Spectroscopy (Bruker XFlash-SDD-5010, Germany).

2.2. Synthesis of MXene $Ti_3C_2T_x$

MXene was synthesized via aqueous acid etching method as previous reported (Mashtalir et al., 2013). First, Ti_3AlC_2 powder (2 g) was slowly added into a mixture of lithium fluoride powders (2 g) and 9 M hydrochloric acid (20 mL). The reaction was kept at 35 °C under magnetic stirring for 24 h. Next, the reaction products were washed with

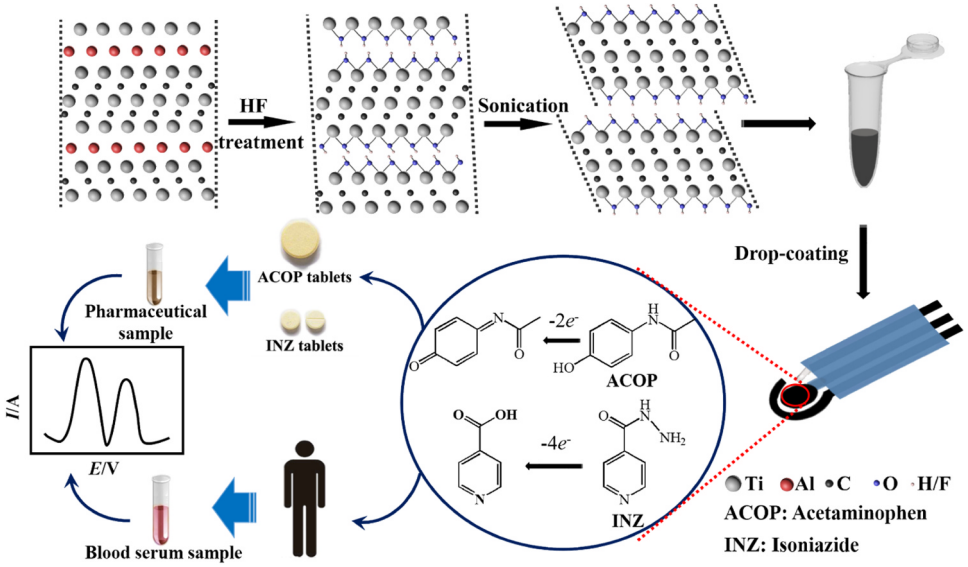

Scheme 1. Schematic diagram of MXene preparation process and electrocatalysis oxidation mechanisms and application of ACOP and INZ detection using SPE/MXene.

ultra-pure water and then centrifuged, after which the supernatant was decanted. The washing process was repeated until the pH of the supernatant reached about 6, and spontaneous delamination of the $Ti_3C_2T_x$ began to occur. The obtained $Ti_3C_2T_x$ sediment was redispersed in ultra-pure water, followed by sonication in a cooling bath at 0 °C for 15 min. The resulting slurry was used without further modification or processing.

2.3. Fabrication of MXene modified screen-printed electrode

Before use, SPEs were activated in 0.1 M NaOH by cyclic voltammetry, which was performed between − 0.3 and + 1.5 V for 40 cycles at a scan rate of 50 mV/s. MXene nanosheets-modified SPE was fabricated by a simple drop-casting process. MXene suspension at 1 mg/mL was first sonicated for 10 min, and a total of 15 μL of the suspension was dropped onto SPE surface and left dry under an infrared light at about 80 °C for 30 min.

2.4. Real samples test

Ten medicinal tablets were precisely weighed and then fully ground. A certain amount of the powder was dispersed in 100 mL distilled water and then stirred and centrifuged at 6000 rpm for 10 min. Afterwards, 2 mL supernatant was taken out and diluted by 100 times with 0.1 M H_2SO_4 for subsequent analysis. Fresh human blood samples were collected from local hospital. Prior to measurement, the samples were centrifuged at 4000 rpm for 10 min and the supernate serum was collected and then diluted 50 times with 0.1 M H_2SO_4. Different amounts of ACOP and INZ were added into the diluted serum samples. Recovery test was carried out by dropping 150 μL of the spiked sample onto MXene/SPE and electrical responses were tracked via differential pulse voltammetry (DPV). The serum samples were stored at − 4 °C when not in use.

3. Results and discussion

3.1. Physicochemical characterization of MXene

Representative SEM image of $Ti_3C_2T_X$ (Fig. 1A) illustrates accordion-like morphology, indicating delaminating structure of MXene particles. EDS spectra in Fig. 1B reveal the composition of Ti_3AlC_2 before and after HF treatment. Certain amount of Al exists in raw material of Ti_3AlC_2, and atomic fraction of Al was decreased obviously after HF etching

(Supporting Information, Table S1). The chemical reaction of Ti_3AlC_2 with HF is shown in Eq. (1) and the following reaction is displayed in Eq. (2). As observed, certain amounts of F atoms are left after HF treatment, which contribute to the constitution of MXene.

$$Ti_3AlC_2 + 3HF = AlF_3 + 3/2\ H_2 + Ti_3C_2 \quad (1)$$

$$Ti_3C_2 + 2HF = Ti_3C_2F_2 + H_2 \quad (2)$$

3.2. Electrochemical characterization of SPE/MXene

CV and EIS tests were carried out to evaluate electrochemical performance of MXene modified SPE in supporting electrolyte. As depicted in Fig. 1C, both oxidation and reduction peak currents from SPE/MXene are higher than that of SPE, which can be ascribed to the high conductivity and large surface area of MXene. Furthermore, potential difference between oxidation and reduction peaks of SPE/MXene is slightly decreased, suggesting that MXene modification elevates the reversibility of redox reactions of $[Fe(CN)_6]^{3-/4-}$. This result illustrates that MXene decorated electrode possesses improved electrochemical property and suitable for electrochemical sensing application. Fig. 1D shows EIS Nyquist plot of SPE and SPE/MXene, where the diameter of the semicircle is associated with the blockage behavior of the electrode surface for the charge transfer to the redox couple, and the plots were

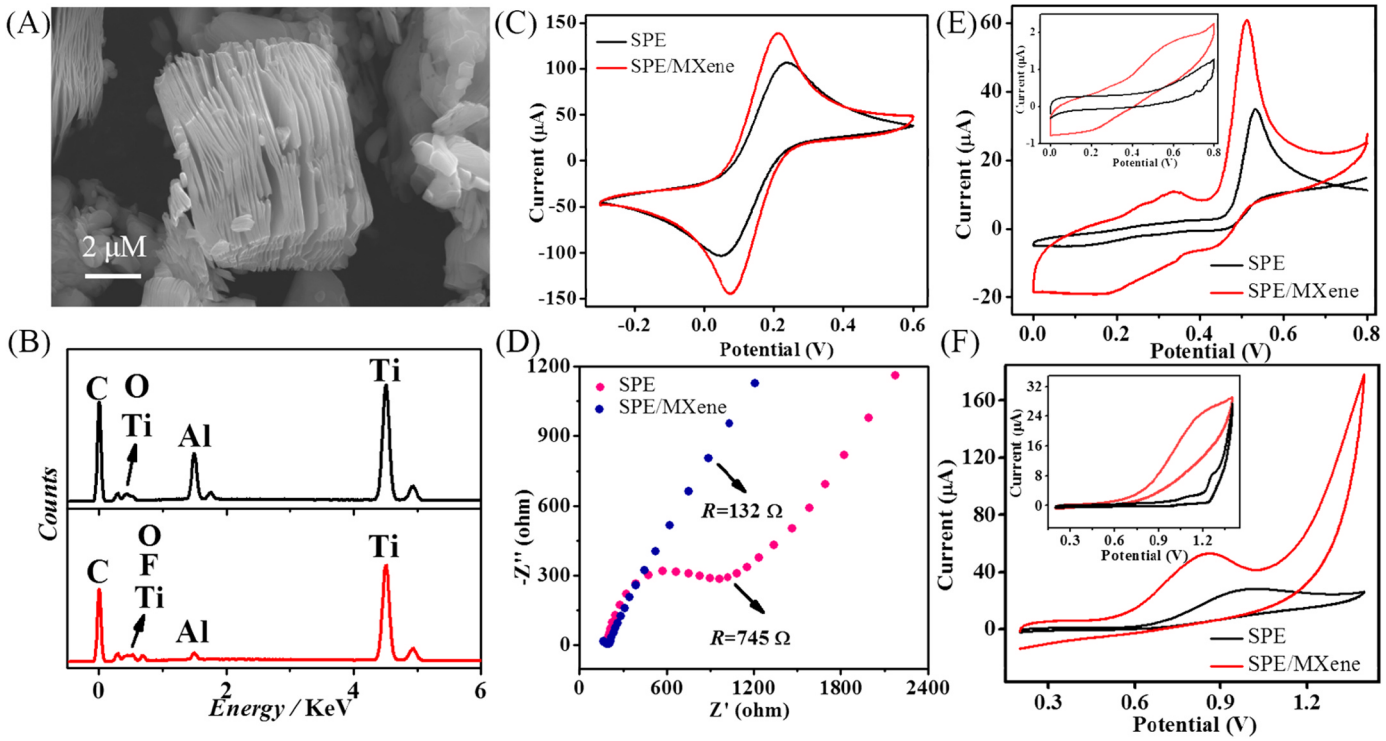

Fig. 1. (A) SEM image of $Ti_3C_2T_x$ and (B) EDS spectra of Ti_3AlC_2 before (black line) and after (red line) HF treatment; Cyclic voltammograms (C) and Nyquist diagrams (D) of SPE and SPE/MXene. Supporting electrolyte contained 5 mM $[Fe(CN)6]^{3-/4-}$ with 0.1 M KCl. Scan rate of CV was 100 mV/s if not specified. Frequency range of EIS was 0.1 Hz~100 kHz. The initialization potential was 0.224 V. Cyclic voltammograms of SPE and SPE/MXene in the presence of 1 mM ACOP (E) and 1 mM INZ (F) in 0.1 M H_2SO_4, respectively. Inset was cyclic voltammograms of SPE and SPE/MXene in 0.1 M H_2SO_4.

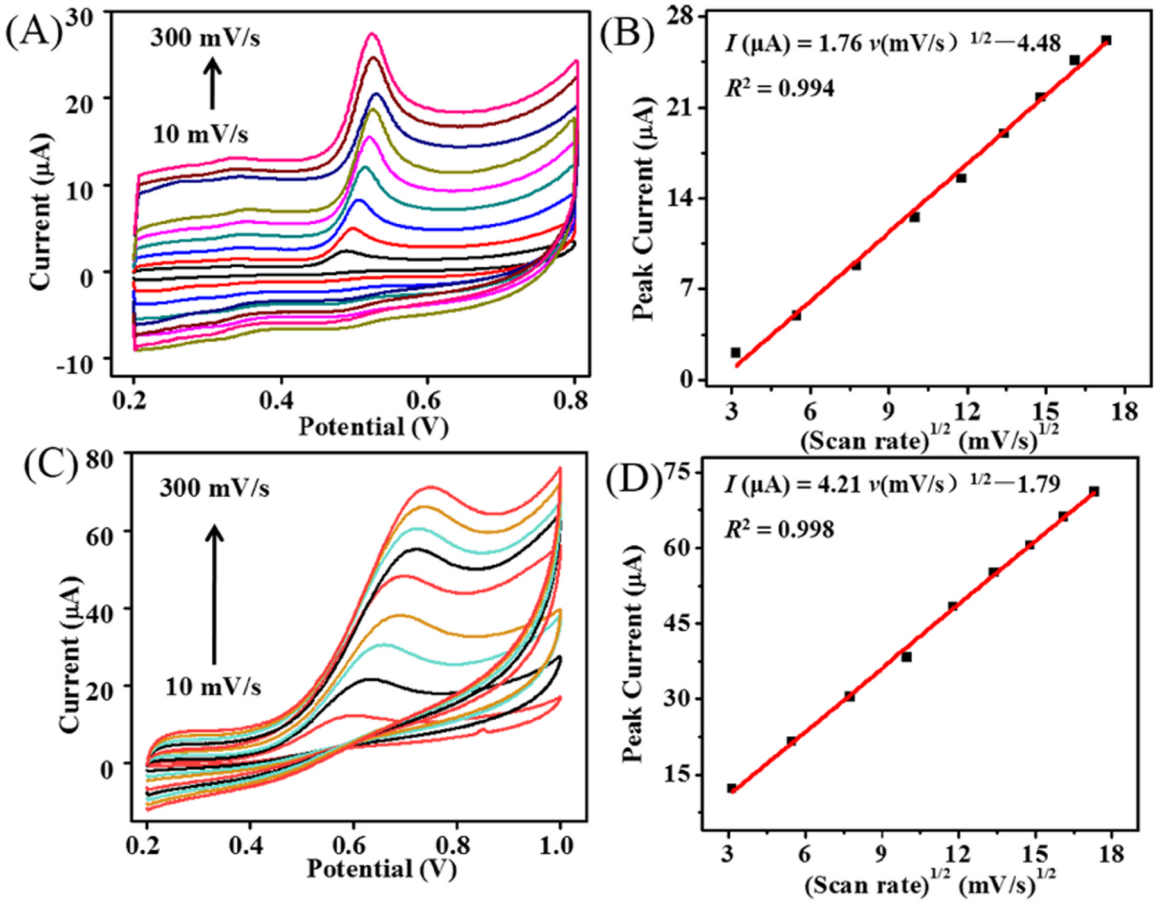

Fig. 2. Cyclic voltammograms of MXene/SPE at different scan rate in 0.1 mM ACOP and oxidation peak currents versus square-root of scan rate plot (A and B) and in 1 mM INZ (C and D). Electrolyte is 0.1 M H_2SO_4.

fitted by the software of Z-view to demonstrate electron-transfer resistance (R) of electrode. As shown, there is an obvious semicircle present at SPE, and R was calculated to be 745 Ω. With MXene modification, the interfacial resistance decreased substantially, and R of SPE/MXene was calculated to be 132 Ω, implying enhanced electron transfer property and better mass transfer performance, which are in consistence with the above results from CV.

3.3. Electrochemical behavior of ACOP and INZ at SPE/MXene

The electrochemical responses of ACOP and INZ were studied in three common electrolytes including 0.1 M H_2SO_4, phosphate buffer (PB, pH 7.4) and NaOH. It turns out that the signals of ACOP and INZ were clearly separated when 0.1 M H_2SO_4 used as electrolyte (Supporting Information, Fig. S1). Oxidation mechanism of INZ and ACOP is shown in Scheme 1, Eq. (3) (Majidi et al., 2006; Yalgudre and Gokavi, 2012) and Eq. (4) (Su and Cheng, 2010). The pK_a value of INZ is about 3.5 (Ràfols et al., 2011), and that of the pyridine nitrogen is reported to be 1.8, implying a further positive charge is present on INZ in condition of 0.1 M H_2SO_4, and its protonation equilibrium was represented in Eq. (3). Positively charged form makes INZ easier to be attracted by the negative charges of MXene/SPE. This is the reason why well-defined current signal of INZ is observed in 0.1 M H_2SO_4. As for ACOP, its pK_a value is about 9.5; in electrolyte with pH > 9.5, ACOP is mainly present in deprotonated form which exhibits a net negative charge, and thus repulsed by the negative charge of the MXene/SPE surface. Therefore, acidic medium (pH lower than its pK_a is ideal for full electrooxidation of ACOP at MXene/SPE. The above results indicate that 0.1 M H_2SO_4 is the suitable medium for electrochemical oxidation of both ACOP and INZ.

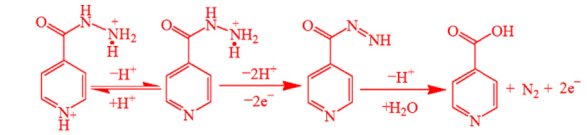

Positively charged INZ (3)

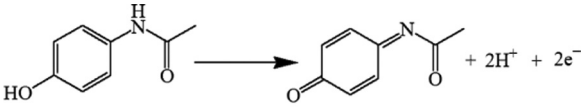

ACOP (4)

Individual CV responses of ACOP and INZ in 0.1 M H_2SO_4 at SPE and MXene/SPE were probed. As can be seen from Fig. 1E and F, no obvious peak current signal of SPE and SPE/MXene was observed in 0.1 M H2SO4 (inset of Fig. 1E and F), and 1 mM ACOP and INZ exhibit oxidation peaks around 0.53 V and 0.95 V at SPE, respectively (Fig. 1E and F). After MXene modification, larger and well-defined peak currents were observed at around 0.50 V for ACOP (Figs. 1E) and 0.85 V for INZ (Fig. 1F) on MXene/SPE (vs Ag/AgCl). The peak potential difference of ACOP and INZ is about 0.35 V that allows simultaneous and selective detection of ACOP and INZ. Compared with bare electrodes, current response of MXene modified electrodes towards both analytes present obvious signal amplification and their oxidation peak potentials are closer to zero, suggesting outstanding catalytic ability of MXene on oxidation reactions of the compounds. The highelectrocatalytic activity of MXene/SPE could be attributed to the accordion-like structure and

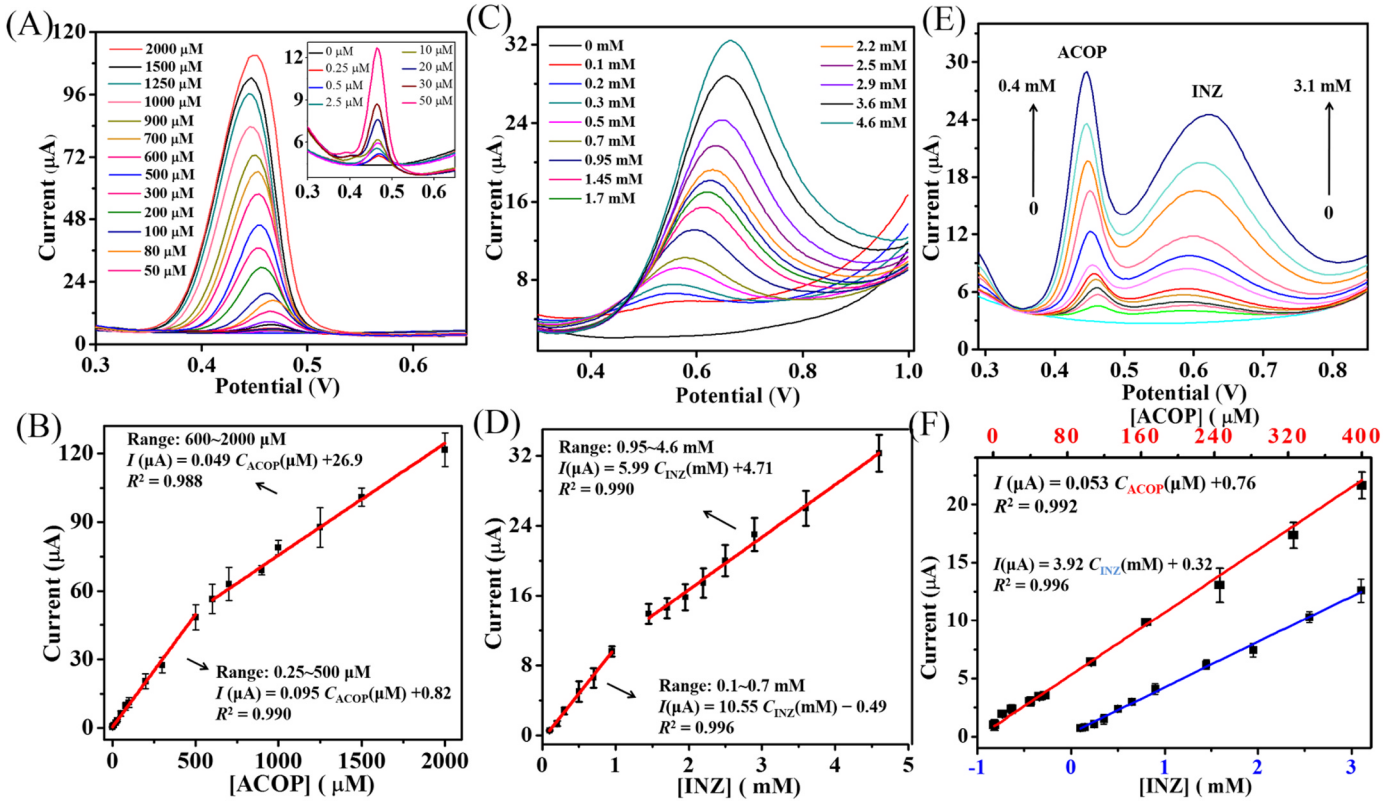

Fig. 3. Differential pulse voltammograms of MXene/SPE to different concentrations of ACOP (A) and INZ (C) in 0.1 M H_2SO_4 and linear relationship between peak currents and concentrations of ACOP (B) and INZ (D) from three parallel tests; Differential pulse voltammograms at MXene/GCE in 0.1 M H_2SO_4 containing different concentrations of ACOP and INZ (E). Linear relationship between the peak current and the concentration of ACOP (red line) and INZ (blue line) from three parallel tests (F). DPV experiments were performed with amplitude of 50 mV. Pulse width and pulse period was 50 ms and 0.5 s, respectively.

good conductivity of MXene, which endows large surface area and accelerates electron transfer, and thus renders MXene ideal in electrochemical detection of ACOP and INZ.

In order to investigate the effect of scan rate, cyclic voltammograms of SPE/MXene were recorded at various scan rates (ν) in the range of 10–300 mV/s (Fig. 2A and B), and oxidative peak current increases linearly with the square root of scan rate, and the corresponding calibration equation is I (μA) = 1.76 ν (mV/s)$^{1/2}$-4.48, R^2 = 0.994 for ACOP, I (μA) = 4.21 ν (mV/s)$^{1/2}$-1.79, R^2 = 0.998 for INZ (Fig. 2C and D). Besides, there was a positive shift of peak potential with the increase of scan rate. The results show that electrochemical oxidation behavior of ACOP and INZ at MXene/SPE is a diffusion controlled electrochemical process.

3.4. Electrochemical detection of ACOP and INZ

3.4.1. Calibration curve in their individual solution

DPV was employed to investigate the sensitivity of MXene/SPEs in terms of linear ranges and detection limits for ACOP and INZ. Fig. 3A and C display the DPV responses of the electrochemical oxidation of ACOP and INZ using MXene/SPE in 0.1 M H_2SO_4. Peak current was increased with continuous addition of ACOP and INZ, and both compounds shows double linear relationships (Fig. 3B and D). Slope of the calibration curves gets smaller at the second concentration segment, demonstrating the reduced sensitivity at higher concentration range. This could be ascribed to the fact that a thicker layer of analyte forms with the increased number of molecules, leading to larger diffusion resistance of the molecules (Saravanan et al., 2017). Besides, coverage of the electrode surface with the reaction products may be also related to the reduce sensitivity (Li et al., 2015). Detection limits of ACOP and INZ were calculated to be 0.048 μM and 0.064 mM (S/N = 3), respectively.

Table 1 is a comparison of ACOP and INZ detection using various electrochemical sensors. It can be found that our presented MXene/SPE features comparable or better performance than other modified electrodes. The enhanced catalytic performance of MXene/SPE may be attributed to the following three reasons: (1) As a titanium-rich material, not only can $Ti_3C_2T_x$ MXenes work as a robust carbon support but effective conductive channels for electrons. (2) The accordion-like layered structure feature for MXenes favors more active sites exposure and facilitates faster transfer for electrolyte and electron during the electrocatalytic process. (3) The obtained $Ti_3C_2T_x$ MXene nanosheets have a negatively charged surface due to the existence of –F, −OH, or =O surface groups, which is beneficial to aggregation of positively charged analytes.

3.4.2. Simultaneous detection of ACOP and INZ

Simultaneous test of ACOP and INZ was carried out by DPV in 0.1 M H_2SO_4. As shown in Fig. 3E, two well-separated and distinct oxidation peaks of ACOP and INZ were observed, and peak currents for the two analytes increase linearly with concentrations without interfering with each other (Fig. 3F). This result verifies the feasibility of simultaneous assay of ACOP and INZ by using MXene/SPE.

3.5. Repeatability and stability of SPE/MXene for ACOP and INZ assay

Reproducibility of MXene/SPE was investigated by using the same electrode for five repetitive measurements of 100 μM ACOP and 1 mM INZ. The relative standard deviation (RSD) was calculated to be 2.2% and 1.6% for ACOP and INZ, respectively. In addition, reproducibility

Table 1
Comparisons of MXene/SPE with previous reported electrochemical methods for ACOP and INZ determinations.

Electrodes	Analyte	Linear range	LOD (μM)	Ref.
[a]CNPs/[b]GCE	ACOP	0.1–100 μM	0.05	(Ghorbani-Bidkorbeh et al., 2010)
MWCNT/[c]PDDA/[d]PSS/[e]GE	ACOP	25–400 μM	0.5	(Manjunatha et al., 2011)
[f]Pt/NGr /GCE	ACOP	0.05–90 μM	0.008	(Anuar et al., 2018)
[g]RGO–Au/GCE	INZ	0.1 μM~1.0 mM	0.01	(Guo et al., 2015)
[h]PdNPs/[i]CILE	INZ	5 μM~2.6 mM	0.47	(Absalan et al., 2016)
[j]PYZ/BPH/GO/PAG/GCE	INZ	20–1400 μM	2.59	(Devadas et al., 2015)
Rh[k]/GCE	INZ	70–1300 μM	13	(Cheemalapati et al., 2014)
MXene/SPE	ACOP	0.25–2000 μM	0.048	This work
	INZ	0.1 ~4.6 mM	64	

Rh[k]: rhodium.
[a] CNPs: carbon nanoparticles.
[b] GCE: glassy carbon electrode.
[c] PDDA: poly (diallyl dimethyl ammonium chloride).
[d] PSS: poly styrene sulfonate.
[e] GE: graphite electrode.
[f] Pt/NGr: platinum nitrogen-doped grapheme.
[g] RGO–Au: reduced graphene oxide (RGO) and Au nanocomposites.
[h] PdNPs: palladium nanoparticles.
[i] CILE: carbon ionic liquid electrode.
[j] PYZ/BPH/GO/PAG/GCE: pyrazinamide and buspirone HCl (BPH) at graphene oxide (GO)/poly- l -arginine (PAG)-modified GC.

Table 2
Determination of ACOP and INZ added in human serum samples using MXene/SPE by DPV (n = 3).

Blood serum	Added (μM)		Found (μM)		Recovery (%)		RSD (%) (n = 3)	
	ACOP	INZ	ACOP	INZ	ACOP	INZ	ACOP	INZ
1	60	250	60.8 ± 2.41	256.3 ± 4.01	101.3	102.5	3.0	1.1
2	180	750	178.4 ± 1.52	743.0 ± 8.10	99.1	99.1	1.2	0.8

was also studied employing five separately produced MXene/SPEs. These electrodes were examined in the presence of 100 μM ACOP and 1 mM INZ under the same conditions, and the RSD obtained were 4.3% for ACOP and 4.1% INZ. These results confirmed that MXene/SPE has good repeatability and reproducibility. Stability evaluation was performed by using the same sensor for continuous and simultaneous analysis of ACOP and INZ every day for sustained two weeks, during which the electrode was stored in air at room temperature. After 2 weeks, the responses of MXene/SPE retained 97.2% and 95.8% of the initial values, and the RSD was 2.7% and 3.5% for ACOP and INZ, respectively, indicating good long-term stability of MXene/SPE. It is worth to mention that, thanks to the good stability of titanium element, $Ti_3C_2T_x$ could efficiently avoid self-corrosion that always happens in noble metal/carbon catalyst.

3.6. Analysis of real samples

3.6.1. Determination of ACOP and INZ in their individual pharmaceutical samples

The constructed sensor was employed to determine the content of ACOP and INZ in their pharmaceutical samples (tablets). Recoveries of the testing results are around 100%. The specific data are listed in Table S2 in the Supplementary information file. This result suggests good accuracy and repeatability of the developed method in real sample analysis.

3.6.2. Simultaneous test of ACOP and INZ in human blood serum

In order to verify the feasibility of the method in clinical application, SPE/MXene was applied for analysis of human blood serum samples. DPV responses of simultaneous detection of ACOP and INZ were presented in Fig. S2, where two separated oxidation peaks were observed. Accuracy was determined by standard addition method and recovery of the spiked samples ranged from 99.1% to 102.5% (Table 2), indicating the detection procedure is free from interferences in blood serum matrix.

4. Conclusion

In summary, we have established a facile and sensitive electrochemical sensor based on MXene modified SPE. It is found that the accordion-like MXene has a high surface area and good conductivity benefiting electron transfer and shows excellent electrocatalytic activity toward oxidation of ACOP and INZ. Clearly separated oxidation peaks of ACOP and INZ were obtained, allowing for simultaneous determination of both analytes by using MXene/SPE. Furthermore, the developed sensor showed good repeatability, reproducibility and stability. More importantly, ACOP and INZ can be gauged in their human serum samples free from significant interference, illustrating the effectiveness and practicability of the proposed sensor. However, a natural drawback, electrode fouling existed in the system. Besides, SPE/MXene exhibits a rather high detection limit of INZ. Further study is in progress to circumvent these drawbacks, including introduction of self-cleaning materials and inner-reference substances, and optimizing the detection conditions. Above all, the sensor exhibits excellent advantages of facile preparation, high catalytic activity, low reagent use and cost effectiveness which make SPE/MXene a promising candidate for therapeutic drug monitoring in clinic.

CRediT authorship contribution statement

Yu Zhang: Conceptualization, Methodology, Software, Data curation, Writing - original draft, Writing - review & editing. **Xiantao Jiang:** Resources, Formal analysis. **Junjie Zhang:** Data curation, Writing - review & editing. **Han Zhang:** Project administration. **Yingchun Li:** Writing - review & editing, Supervision.

Acknowledgments

The authors are grateful to the National Natural Science Foundation of China (81773680) and free exploration project from the Natural Science Foundation of Shenzhen (JCYJ20170811152540640).

Declaration of interests

The authors declare that they have no known competing financial interests or personal relationships that could have appeared to influence the work reported in this paper.

Appendix A. Supporting information

Supplementary data associated with this article can be found in the online version at doi:10.1016/j.bios.2019.01.043.

References

Absalan, G., Akhond, M., Soleimani, M., Ershadifar, H., 2016. J. Electroanal. Chem. 761, 1–7.
Ahmed, M.U., Hossain, M.M., Safavieh, M., Wong, Y.L., Rahman, I.A., Zourob, M., Tamiya, E., 2015. Crit. Rev. Biotechnol. 36 (3), 495–505.
Ampolson, L., 2006. Dig. World Core Med. J. 43 (4), 1364–1372.
Anuar, N.S., Wan, J.B., Ladan, M., Shalauddin, M., Mehmood, M.S., 2018. Sens. Actuators B-Chem. 266, 375–383.
Cheemalapati, S., Chen, S.M., Ali, M.A., Al-Hemaid, F.M.A., 2014. Colloid Surf. B 121 (9), 444–450.
Cheng, H., Wang, X., Wei, H., 2015. Anal. Chem. 87 (17), 8889–8895.
Devadas, B., Cheemalapati, S., Chen, S.M., Ali, M.A., Al-Hemaid, F.M.A., 2015. Ionics 21 (2), 547–555.
Epstein, M.M., Nelson, S.D., Slattery, J.T., Kalhorn, T.F., Wall, R.A., Wright, J.M., 2012. J. Clin. Pharmacol. 31 (2), 139–142.
Espinosa, B.M., Ruiz Sánchez, A.J., Sánchez, R.F., Bosch, O.C., 2006. J. Pharm. Biomed. 42 (3), 291–321.
Fernandes, G.F.D.S., Salgado, H.R.N., Santos, J.L.D., 2017. Crit. Rev. Anal. Chem. 47, 136–144.
Gao, G., O'Mullane, A.P., Du, A., 2017. Acs Catal. 7 (1), 494–500.
Ghorbani-Bidkorbeh, F., Shahrokhian, S., Mohammadi, A., Dinarvand, R., 2010. Electrochem. Acta 55 (8), 2752–2759.
Guo, Z., Wang, Z.Y., Wang, H.H., Huang, G.Q., Li, M.M., 2015. Mater. Sci. Eng. C 57, 197–204.
Hantanasirisakul, K., Zhao, M.Q., Urbankowski, P., Halim, J., Anasori, B., Kota, S., Ren, C.E., Barsoum, M.W., Gogotsi, Y., 2016. Adv. Electron. Mater. 2 (6), 1–7.
Kullakublick, G.A., Andrade, R.J., Merz, M., End, P., Benesic, A., Gerbes, A.L., Aithal, G.P., 2017. Gut 66 (6), 1154–1164.
Kumar, S., Lei, Y., Alshareef, N.H., Quevedo-Lopez, M., Salama, K.N., 2018. Biosens. Bioelectron. 121, 243–249.
Lawrence Goldkind, M.D., Loren Laine, M.D., 2010. Pharmacoepidemol. Drug Saf. 15 (4), 213–220.
Leitner, J.M., Graninger, W., Thalhammer, F., 2010. Infect 38 (1), 3–11.
Li, Y., Liu, Y., Yang, Y., Yu, F., Liu, J., Song, H., Liu, J., Tang, H., Ye, B.C., Sun, Z., 2015. Acs Appl. Mater. Interfaces 7 (28), 15474–15480.
Lukatskaya, M.R., Mashtalir, O., Ren, C.E., Dall'Agnese, Y., Rozier, P., Taberna, P.L., Naguib, M., Simon, P., Barsoum, M.W., Gogotsi, Y., 2013. Science 341 (6153), 1502–1505.
Majidi, M.R., Jouyban, A., Asadpour-Zeynali, K., 2006. J. Electroanal. Chem. 589 (1), 32–37.
Manjunatha, R., Suresh, G.S., Melo, J.S., D'Souza, S.F., 2011. Electrochim. Acta 56 (19), 6619–6627.
Mashtalir, O., Naguib, M., Dyatkin, B., Gogotsi, Y., Barsoum, M.W., 2013. Mater. Chem. Phys. 139 (1), 147–152.
Nolan, C.M., Goldberg, S.V., Buskin, S.E., 1999. J. Am. Med. Assoc. 281 (11), 1014–1018.
Ràfols, C., Bosch, E., Ruiz, R., Box, K.J., Reis, M., Ventura, C., Santos, S., Araújo, M.E., Martins, F., 2011. J. Chem. Eng. Data 57 (2), 330–338.
Rakhi, R.B., Ahmed, B., Hedhili, M.N., Anjum, D.H., Alshareef, H.N., 2015. Chem. Mater. 27 (15), 5314–5323.
Rumack, B., Heard, K., Green, J., Albert, D., Bucher-Bartelson, B., Bodmer, M., Sivilotti, M.L., Dart, R.C., 2012. J. Hum. Pharmacol. Drug Ther. 32 (9), 784–791.
Saravanan, J., Ramasamy, R., Therese, H., Amala, G., George, G.K., 2017. New J. Chem. 41 (23), 14766–14771.
Shahrokhian, S., Amiri, M., 2007. Microchim. Acta 157 (3–4), 149–158.
Su, W.Y., Cheng, S.H., 2010. Electroanalysis 22 (6), 707–714.
Tan, K., Ma, Q., Luo, J., Xu, S., Zhu, Y., Wei, W., Liu, X., Gu, Y., 2018. Biosens. Bioelectron. 117, 713–719.
Tang, Q., Zhou, Z., Shen, P., 2012. J. Am. Chem. Soc. 134 (40), 16909–16916.
Yalgudre, R.S., Gokavi, G.S., 2012. Ind. Eng. Chem. Res 51 (14), 5135–5140.
Zhu, J., Ha, E., Zhao, G., Zhou, Y., Huang, D., Yue, G., Hu, L., Sun, N., Wang, Y., Lee, L.Y.S., 2017. Coord. Chem. Rev. 352, 306–327.